Examining the Pearlite Growth Interface in a Fe-C-Mn Alloy

R. E. Waters, M. J. Whiting, and V. Stolojan

Abstract—A method of collecting composition data and examining structural features of pearlite lamellae and the parent austenite at the growth interface in a 13wt. % manganese steel has been demonstrated with the use of Scanning Transmission Electron Microscopy (STEM). The combination of composition data and the structural features observed at the growth interface show that available theories of pearlite growth cannot explain all the observations.

Keywords—Interfaces, Phase transformations, Pearlite, Scanning Transmission Electron Microscopy (STEM).

I. INTRODUCTION

PEARLITE is defined as a lamellar product of eutectoid decomposition and a vast body of work, concerning its growth mechanism, has been published since it was first observed by Henry Clifton Sorby in 1886 [1]. The area that has created the most debate is the interface between the growing lamellar phases and the parent phase into which they are growing. There are essentially two approaches to explain the necessary atomic-scale processes that occur at the growth interface. One approach is an atom by atom addition to the product phases, the Zener-Hiller approach [2]-[4], and the other a ledge mechanism in which atoms arrive at ledge risers [5], [6]. One of the main problems in understanding the precise nature of the growth process is the lack of accurate data on the composition of the parent phase and the pearlite phases close to the growth front. A number of studies [7]-[14], have attempted to measure the compositions close to the growth front but due to the preparation techniques of the specimens examined and analytical methods used to gather the data, the results were of limited spatial resolution. The purpose, therefore, of the present work is to conduct an investigation on a high wt.% Mn Fe-C-Mn alloy subjected to an isothermal heat treatment, and with the use of high spatial resolution Scanning Transmission Electron Microscopy, measure the composition across the growth front in thin foil samples.

R. E. Waters is with the Department of Engineering Materials, University of Surrey, Guildford, Surrey, GU2 7XH (phone:+44(0)1483-689476; e-mail: r.waters@surrey.ac.uk).

M. J Whiting is with the Department of Engineering Materials, University of Surrey, Guildford, Surrey, GU2 7XH (e-mail: m.whiting@surrey.ac.uk).

V. Stolojan is with the Advanced Technology Institute, University of Surrey, Guildford, Surrey, GU2 7XH (e-mail: v.stolojan@surrey.ac.uk).

II. EXPERIMENTAL PROCEDURE

A. Material

The alloy selected for the investigation was a high manganese Fe-C-Mn alloy with a composition of approximately 13wt. % Mn and 0.8wt. % C. The reason for the selection of this alloy is that similar alloys have been used previously [5], [15], [16], in investigating various aspects of pearlite nucleation and growth. The alloy is also especially suitable for the study of pearlite as it produces a eutectoid lamellar structure in contact with the parent phase, which is metastable at room temperature. This is achieved by the manganese depressing the phase transformation temperatures, so when quenching from the γ-region it is possible to obtain metastable austenite as the M_s temperature is below room temperature.

B. Sample Preparation

The heat treatments were carried out on $10 \times 15 \times 5$mm samples cut from strips of the bulk material. The samples were solution treated at 1000°C for 10min and quenched in water. Following solution treatment, the samples were subjected to isothermal heat treatment at a temperature of 640°C. During the isothermal heat treatment, samples were removed at allocated time intervals and quenched in water to halt the transformation. Following the isothermal heat treatments, sections were cut from the samples and mounted, ground and polished using standard techniques. To allow for the inspection of the microstructural evolution, specimens were etched with 2% nital and examined using both reflected light microscopy and scanning electron microscopy.

To determine the volume fraction of pearlite, standard point counting was used by overlaying a grid consisting of 100 points on images captured using a Zeiss Axiophot microscope. For each sample a minimum of 10 images were collected, the volume fraction was calculated for each image then averaged for each sample. Due to the limited resolution of the light microscope, further examination of the samples was conducted using a Hitachi S-3200N SEM to observe the morphology of the pearlite colonies.

For Scanning Transmission Electron Microscopy (STEM), thin foils were created by sectioning slices with a diamond wheel with a constant flow of lubrication to minimise specimen heating. After sectioning, foils were mounted onto a brass polishing jig using wax and ground to approximately 80 μm using wet 800 SiC grit paper. Following the grinding of the thin foils, 3mm discs were punched from the foils.

The 3mm discs were electropolished in a StruersTenupol™ twin jet electropolisher using a variety of electrolytes. The electrolytes selected were a solution of 5% perchloric acid in acetic acid at 30V with the solution at room temperature, this is the same procedure used by Lee and Park [17]. The same solution was used with different operating parameters, the temperature of the electrolyte was controlled to maintain 16 °C at an operating voltage of 37V as this had been used by Zhang and Kelly [18]. An alternative electrolyte was used of 1% perchloric acid in methanol at a current of 20mA operating at -20°C as in the study by Zhou and Shiflet [16].

An alternative preparation method involving ion beam thinning was also used. From the foils, 3mm discs were mechanically punched and attached to slotted grids and then ground and polished to approximately 30-50μm. The specimens were then ion polished using a Gatan Precision ion Polishing (PiPs™) machine operating at a beam energy of 5 kV with a milling angle of 5°.

A Hitachi HD 2300A STEM operating at 200kV and equipped with an EDAX Genesis system was used for all the thin foil characterisation reported here. For each sample examined, once a colony had been located, the specimen was oriented so the growth interface was parallel to the incident beam and the ferrite/cementite lamellar interfaces were as near parallel to the beam as possible. For the collection of the x-ray data, a line profile was created so that it crosses the parent/growing phase interface. Several line profiles were obtained for each lamella, typically ranging from 800nm to 60 nm in length, each consisting of at least 5 data points. This approach gave several spectra along the lamellae, across the growth interface and into the parent phase.

C. Data Quantification

Quantification was only attempted for the substitutional elements (Fe and Mn), the reason for this is due to the difficulties in collecting reliable and reproducible data for carbon in STEM thin foils.

For quantification of the x-ray spectra, a software package using MThin was used that operates based on the standard Cliff-Lorimer [19] ratio approach using sensitivity factors, k, according to relationships of this form:

$$\frac{c_{Fe}}{c_{Mn}} = k \frac{I_{Fe}}{I_{Mn}} \qquad (1)$$

where I is the number of counts in the Kα peak of the spectra, C is the weight percent of the substitutional elements and *k* is the Cliff-Lorimer factor or can be referred to as a sensitivity factor.

The k factor varies based on the STEM and EDS system used and the accelerating voltage the STEM is operating at. The samples were thin enough for the effects of absorption and fluorescence to be ignored; therefore the sensitivity factor is only related to the atomic-number correction factor (Z) and is assumed not to be dependent on small local changes in thickness. To determine the sensitivity factor, k, and to test the assumption that absorption or fluorescence effects could be ignored, an as-quenched sample was used as a reference. For all of the profiles a beam size of approximately 1nm and a 'live' x-ray acquisition time of 10 seconds were used, this resulted in a consistent k value of 1.04.

III. RESULTS AND DISCUSSION

A. Microstructure

By plotting the volume fraction transformed (V_f), for all the isothermal treatments as a function of treatment duration (Fig. 1) it is possible to see that the volume fraction transformed increases, as the duration increases, as expected. On this basis it was determined that a specimen that had been treated for 8 hours would be examined by STEM as the resulting 8% volume fraction transformed is at the mid-point of the pearlite transformation (on completion this steel would have c. 15% pearlite).
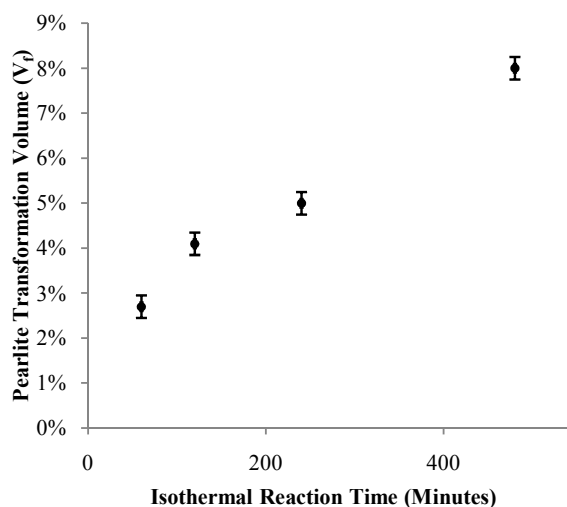

Fig. 1 Plot of pearlite transformation volume (V_f) as a function of treatment time

During the study of the microstructure using light microscopy, the pearlite regions nucleated mainly on specific prior austinite grain boundaries. Some of the colonies were not resolvable with light microscopy, therefore the use of SEM was needed to discern the lamellae. The morphology of a typical pearlite colony is illustrated in Fig. 2.
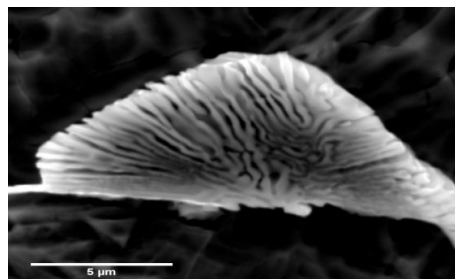

Fig. 2 SEM secondary electron images of a pearlite colony, after heat treatment at 640°C for 8hr

B. Scanning Transmission Electron Microscopy (STEM)

For analysis of the growth interface, specimens prepared using PiPs were selected. The benefit of using ion polishing compared to electropolishing is that the specimen is thinned uniformly, whilst electropolishing had a tendency to preferentially thin the ferrite. There was a value in thinning by both an ion beam method and electropolishing and cross-checking the results, as both techniques can introduce artifacts.

Everal interfaces were investigated, with profiles taken for both γ/α and γ/Fe$_3$C interfaces. An example of the typical Mn profile across a γ/α interface, with a corresponding Bright Field (BF) micrograph, is shown in Fig. 3. Each profile line consisted of 5 points and multiple lines were collected for each lamellae.
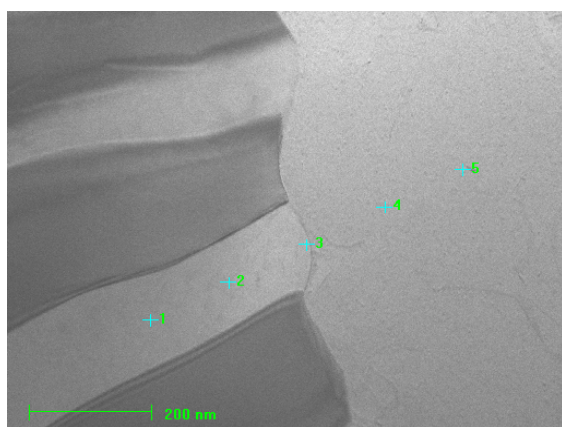
(a)
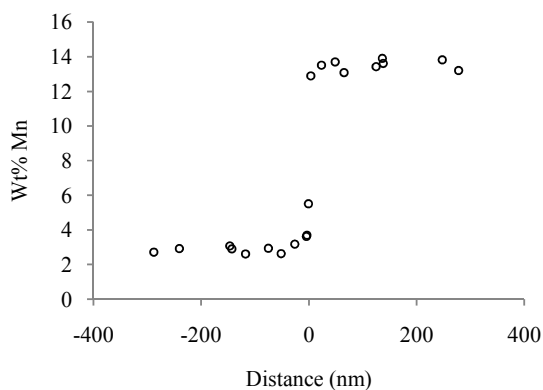
(b)

Fig. 3 (a) BF STEM micrograph of the ferrite/austenite growth interface in a sample treated at 640°C for 8 hr, (b) plot of the Mn profile across the ferrite/austenite growth interface in (a)

The chemical profiles across the pearlite growth interface, for the chosen heat treatment, revealed important information about the phase compositions. The experimental set-up produced a clear set of composition data across the growth front, with the compositions close to the equilibrium values from the phase diagram [20]; the transformation occurs with significant partitioning across the growth interface for the ferrite to austenite.

Along with composition profiles, several micrographs of the growth front are shown in Figs. 4 and 5.
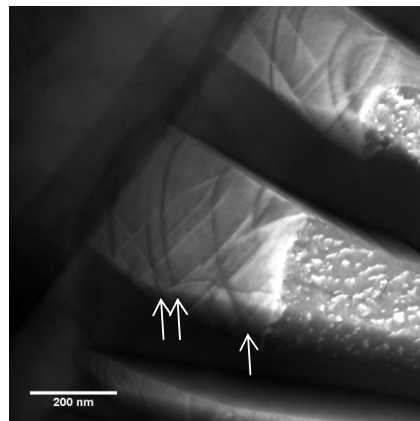

Fig. 4 Bright field image of steps along the growth interface between the ferrite/austenite phases as indicated by the arrows
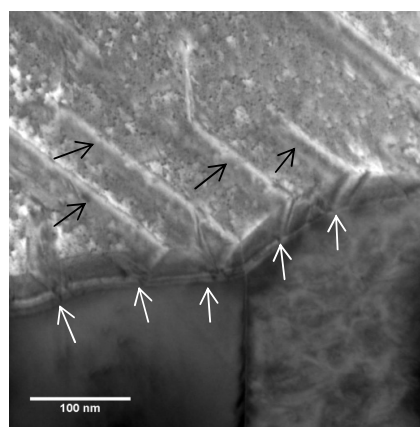

Fig. 5 Bright field image of steps along the growth interface between the ferrite/austenite phases and cementite/austenite phases as indicated by the white arrows. Notice that each step on the interface is associated to a fault in the austenite ahead of the growth front as indicated by the black arrows

From Figs. 4, 5, it can be observed that the growth interface is facetted and what appear to be ledges or steps are present, similar to those noted in other studies [5], [16], [21], [22]. It was generally the case that the 'ledges' were associated with stacking faults in the parent austenite. A similar observation was first made by Khalid and Edmonds [21].

This observation seems to agree with Khalid and Edmonds claim that the steps at the pearlite growth interface are not growth ledges. It should be noted that just because the identified steps are not growth ledges this does not mean that crystallography is unimportant in the growth process. For example, the presence of facets at the growth interface undermines the very basis of the Zener-Hillert approach as the smooth interfacial curvature necessary for the operation of the

Gibbs-Thomson effect is clearly not present at the lamellae tips.

IV. CONCLUSION

The understanding of the growth mechanism of pearlite is a complex subject that is still not fully explained. Neither the classic Zener-Hillert approach nor the more recent ledge mechanism, proposed by Hackney and Shiflet, explain all the available data. The use of STEM enables compositional data to be obtained at a high spatial resolution. Such data is often lacking when growth models are tested. Such data will be useful in testing future models which can account for all the features of the pearlite transformation.

ACKNOWLEDGMENT

REFERENCES

[1] H. C. Sorby, "On the microscopic structures of iron and study of microscopic structures of steel," *J. Iron and Steel Inst.,* vol. 1, pp. 140, 1886.
[2] C. Zener, "Kinetics of the decomposition of austenite," *Trans. Met. Soc. AIME.,* vol. 167, pp. 550, 1945.
[3] M. Hillert, "The formation of pearlite," in *Decomposition of austenite by diffusional processes*, F. Zackay and H. I. Aaronson, Ed. John Wiley New York, 1962, pp. 197.
[4] M. Hillert, "On theories of growth during discontinuous precipitation," *Metall. Trans.,* vol. 3, pp. 2729. 1972.
[5] S. A. Hackney and G. J. Shiflet, "Pearlite growth mechanism," *Acta. Metall.,* vol. 35, pp. 1019, 1987.
[6] M. J. Whiting and P. Tsakiropoulos, "Ledge mechanism of pearlite growth: growth velocity of ferrous pearlite," *Mater. Sci. Technol.,* vol. 11, pp. 977, 1995.
[7] S. A. Al-Salman and N. Ridley, "Partitioning of nickel during pearlite growth," *Scr. Metall.,* vol. 18, pp. 789, 1984.
[8] S. A. Al-Salman, G. W. Lorimer and N. Ridley, "Partitioning of silicon during pearlite growth in a eutectoid steel," *Acta Metall.,* vol. 27, pp. 1391, 1979.
[9] S. A. Al-Salman, G. W. Lorimer and N. Ridley, "Pearlite growth kinetics and partitioning in a Cr-Mn eutectoid Steel." *Metall. Trans. A,* vol. 10, pp. 1703, 1979.
[10] J. Chance and N. Ridley, "Chromium partitioning during isothermal transformation of a eutectoid steel," *Metall. Trans. A,* vol. 12A, pp. 1205, 1981.
[11] N. A. Razik, G. W. Lorimer and N. Ridley, "An investigation of manganese partitioning during the austenite-pearlite transformation using analytical electron microscopy," *Acta Metall.,* vol. 22, pp. 1249, 1974.
[12] N. A. Razik, G. W. Lorimer and N. Ridley, "Chromium partitioning during the austenite pearlite transformation," *Metall. Trans. A,* vol. 7, pp. 209, 1976.
[13] N. Ridley and D. Burgess, "Partitioning of Co during pearlite growth in a eutectoid steel," *Metal Science,* vol. 18, pp. 7, 1984.
[14] N. Ridley, M. A. Malik and G. W. Lorimer, "Partitioning and pearlite growth kinetics in a Ni-Cr eutectoid steel," *Mater. Charact.,* vol. 25, pp. 125, 1990.
[15] R. J. Dippenaar and R. W. K. Honeycombe, "The crystallography and nucleation of pearlite," *Proc. R. Soc. A,* vol. 333, pp. 455, 1973.
[16] D. S. Zhou and G. J Shiflet, "Interfacial steps and growth mechanism in ferrous pearlite," *Metall. Trans. A,* vol. 22A, pp. 1394, 1991.
[17] D. L. Lee and C. G. Park, "Sequential branching by ledge migration for the sidewise growth of pearlite," *Scr. Metall. Mater.,* vol. 32, pp. 907, 1995.
[18] M-X. Zhang and P. M. Kelly, "The morphology and formation mechanism of pearlite in steels," *Mater. Charact.,* vol. 60, pp. 545, 2009.
[19] G. Cliff and G. W. Lorimer, "The quantitative analysis of thin specimens," *J. Micro.,* vol. 103, pp. 203, 1975.
[20] G. Raynor, "Phase equilibria in iron ternary alloys: a critical assessment of experimental literature," *Inst. Metals,* pp. 174, 1988.
[21] F. A. Khaild and D. V. Edmonds, "Observations concerning transformation interfaces in steel," *Acta Metall.,* vol. 41, pp. 3421, 1993.
[22] T. Chairuangsri and D. V. Edmonds, "The precipitation of copper in abnormal ferrite and pearlite in hyper-eutectoid steels," *Acta Mater.,* vol. 48, pp. 3931, 2000.